EXTRACTING THE APPARENT MOTION FROM TWO SUCCESSIVE EIT IMAGES

Samuel F. Gissot[1,*], J.-F. Hochedez[1], F. Dibos[2], R. Brajša[3], L. Jacques[4], D. Berghmans[1], A. Zhukov[1], F. Clette[1], H. Wöhl[3], and J.-P. Antoine[4]

[1]Solar Physics Dept., Royal Observatory of Belgium, 1180 Brussels, Belgium
[*]Tel: +32 2373 0237, Fax: +32 2374 9822, sgissot@oma.be
[2]CEREMADE, Université Paris IX Dauphine, 75775 Paris, France
[3]Kiepenheuer-Institut für Sonnenphysik, 79104 Freibourg, Germany
[4]Institut de physique théorique, UCL, 1348 Louvain-la-Neuve, Belgium

ABSTRACT

The EIT observations cover more than seven years of the 23rd solar cycle. The main synoptic dataset, usually refered to as the "CME Watch", is a nearly uninterrupted sequence of images taken in the Fe XII bandpass at a cadence of four images per hour. In this work we study motion tracking methods in order to estimate displacements from frame to frame. We have implemented a novel optical flow algorithm, and tested it on a couple of successive images. We have linked the apparent motion occuring between two frames to the expected rotation rate. On this short time scale (20 minutes), we are able to retrieve the global parameters of the solar differential rotation. A strategy for the extraction of region with reliable motion will be discussed.

Key words: EIT; differential rotation; motion analysis; optical flow.

1. INTRODUCTION

Since the beginning of the SoHO mission, the EIT archive covered more than half of the 23rd solar cycle. There are three recurrent modes of observations with the EIT instrument onboard SoHO: the synoptic mode, the shutterless, and the "CME Watch" mode. The latter provides nearly uninterrupted sequences in the Fe XII bandpass, at the wavelength of 19.5 nm, at a cadence of approximatively four images per hour. Such a huge archive requires a systematic analysis. New image processing techniques have been recently elaborated to extract small-scale features (Hochedez et al, 2001) from every single image. It is now possible to derive the statistical trends of these small coronal objects along the solar cycle (Hochedez et al, 2002). But many weak coronal objects are better observed in series of images, because of their persistance over time. Hence motion analysis can help coronal physics. The solar corona undergoes a differential rotation. In Brajša et al (2002), the differential rotation has been analyzed using special coronal objects such as bright points, small loops, and point-like structures in the Fe XV line at 28.4 nm, over the time scale of one day. They are detected with interactive or automatic methods (Brajša et al, 2001). Their rotational and meridional motions are derived, and used for a study of the plasma flows in the corona (Vršnak et al, 2003). This yields a sparse velocity field. Our objective is to compute a denser velocity field, not depending on the selection of coronal objects, on short time scale (the time between two images of the "CME Watch"). The differential rotation is subsequently retrieved from our velocity field, and plays the role of a calibration data as well. There are different techniques to compute a dense flow of velocity vectors between two images. Among them, the local correlation technique has been used by November & Simon (1988) on photospheric sequences, but it appeared to be unreliable on an EIT complex signal. In this paper, we use the optical flow (OF) method to compute the velocity field between only two successive images. It provides one velocity vector per pixel. In this technique, it is assumed that the change of intensity between two successive images are driven only by the motion of the emission sources. A second assumption is that the motion is locally uniform, as if the signal was translated in the plane of the image (at least locally). The first assumption is violated when the emission along a given line-of-sight is variable. In the solar corona, this is often the case because of the strong magnetic activity. We thus have added a multiresolution constraint that makes the algorithm more robust to the changes of intensity. Furthermore, for our time scales, the assumption of local uniform translation is acceptable, albeit depending on the location on the solar disk: closer to the limb, the area around the pixel where this assumption holds vanishes.
The resulting field estimates the displacement occuring between the two frames. The existence of bands in latitude of slower or faster rotating plasma with

respect to the mean differential rotation, torsional oscillations (Howard & Labonte, 1980) in the solar EUV corona (19.5 nm), and other solar physics issues will not be discussed in this work. Here, we focus on the study of the differential rotation at the short time scale (20 minutes between two frames). We then propose a strategy to select the regions that have a reliable motion, for a further physical interpretation of the velocity field.

2. THE MOTION ESTIMATION METHOD

The 2D apparent motion field is the projection in the image plane of the 3D velocity field of the moving coronal plasma. We distinguish between three different velocity vector fields:

- the 3D motion (real),
- the apparent motion (projected speed in image plane),
- estimation of the apparent motion: the optical flow quantity.

The 3D motion is well defined when the emitting source is opaque, but the corona is optically thin: the source of emitting radiative flux is not well defined over the line-of-sight. The photon flux is integrated along the optical path in the coronal plasma. This effect of transparency should be kept in mind in the interpretation of the velocity fields.
Here we note I the intensity of the image, $\vec{x} = (x, y)^T$ (index T means transpose) is the location of a pixel, and t is the time variable. In the optical flow method that we use, the motion $\vec{v}(\vec{x}, t)$ is computed from the intensities of this pixel neighborghood in the images at time t and time $t + \delta t$.

2.1. The Brightness Constancy Assumption

The principle of the optical flow technique is based on the assumption that the brightness pattern of the image is constant during the sequence. This assumption is usually refered to as the Brightness Constancy Assumption (BCA). This assumption can be written as:

$$\frac{dI}{dt}(\vec{x}(t), t) = 0 \tag{1}$$

2.2. Optical Flow Gradient Constraint

If we write equation 1 in terms of partial derivatives, taking into account the dependance of I on $\vec{x}$ (spatial coordinates) and t (the temporal variable), as well as the dependance of x on the time t, we get:

$$\frac{dI}{dt}(\vec{x}(t), t) = \frac{\partial x}{\partial t} \times \frac{\partial I}{\partial x} + \frac{\partial y}{\partial t} \times \frac{\partial I}{\partial y} + \frac{\partial I}{\partial t} \tag{2}$$

The brightness constancy assumption finally gives, for each pixel $\vec{x}$ of an image I:

$$\vec{\nabla} I \cdot \vec{v} + I_t = 0 \tag{3}$$

where

$$\vec{v} = (v_x, v_y)^T = (\frac{\partial x}{\partial t}, \frac{\partial y}{\partial t})^T, \tag{4}$$

$$\vec{\nabla} I = (\frac{\partial I}{\partial x}, \frac{\partial I}{\partial y})^T, \tag{5}$$

$$I_t = \frac{\partial I}{\partial t} \tag{6}$$

For the computation of the spatial derivatives, we use robust kernel of convolution (finite difference with implicit interpolation). Temporal derivative is estimated by a forward finite difference (difference of the two successive images). Unfortunately, the BCA only provides one equation for two unknowns per pixel (the two components of the velocity vector). This is the well known aperture problem (one equation, two unknowns). In order to solve aperture, we use the Lucas-Kanade algorithm.

2.3. Lucas-Kanade Algorithm

In the Lucas-Kanade (LK) algorithm (Lucas & Kanade, 1981), a local uniformity of the velocity field is assumed. For a given neighborhood $N_{\vec{x}}$ of a pixel located at $\vec{x}$, we define a linear system of N optical flow equations, one per each pixel in $N_{\vec{x}}$. This linear system is solved by minimizing an energy E_I:

$$\mathbf{v}_{LK} = \underset{\vec{v} \in V}{argmin}\ E_I(\vec{v}) \tag{7}$$

where

$$E_I(\vec{v}) = \sum_{\vec{x} \in N_{\vec{x}}} (\nabla \vec{I} \cdot \vec{v} + I_t)^2 \tag{8}$$

Equations (7) and (8) can also be seen as a Taylor development of a local correlation energy to be minimized, for small temporal shifts δt:

$$\underset{v_x, v_y}{min} \sum_{\vec{x} \in N_{\vec{x}}} (I(x + v_x \delta t, y + v_y \delta t, t + \delta t) - I(x, y, t))^2 \tag{9}$$

For the purpose of improving our motion analysis tool, we introduced a new contraint that makes the algorithm more robust to the intensity variations that are not caused by the motion of the emitting coronal source.

2.4. The Multiresolution Constraint

When using the multiresolution constraint in motion analysis, one assumes that the correct motion, *i.e.* the best approximation of the apparent motion, is

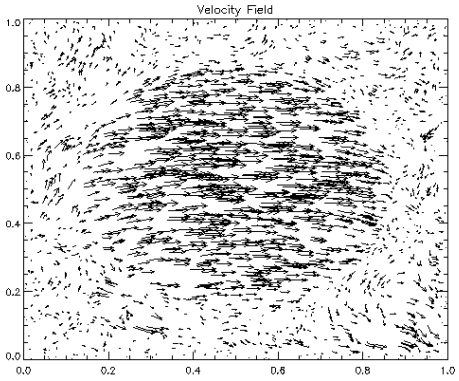

Figure 1. Representation of the velocity vectors estimated with our LK-algorithm (at randomly selected pixels).

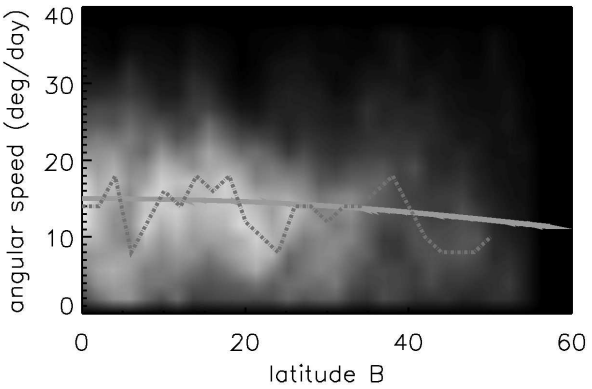

Figure 2. Angular rotation velocity of the pixels in function of latitude. Grey level represents density of pixels, in bins of 2 degrees (latitude) by 2 degrees per day (angular velocity). Full line: fit with a function $f(B) = a + b * sin(B)^2 + c * sin(B)^4$. Dashed line: maxima of pixel density.

accessible at large scales (when the image is subsampled). The finer scales (larger resolution of the image), are used to refine the coarse motion computed at the largest scale. As we are trying to cope with spatially localized variations of intensity, we use a gaussian pyramid for our multiresolution scheme. Thus, we not only subsample our image by a factor 2 to get a larger scale, but we also apply a low-pass filter to the image before the subsampling, so that the influence of intensity variations on the motion estimation diminishes. This improves the algorithm robustness. Indeed the computed velocities are then closer to what is expected from our knowledge of the solar differential rotation.

3. EIT ANALYSIS

We applied our algorithm to a sequence of May 5, 1998 from the "CME Watch" mode of observation. Here we illustrate the ability of our algorithm to analyze the motion occuring between only two images separated by circa 20 minutes (images respectively taken at 20h43min28s UT and 21h04min09s UT). The velocity computed is represented in Figure 1. The time of computation of one velocity field between two images of 1024×1024 pixels is about 5 minutes.

3.1. Retrieving the Differential Rotation

We converted the instantaneous velocity vectors into angular rotation speeds along parallels with correction of $b0$. Meridional drifts are not analyzed here. In Figure 2, the angular velocity of rotation is plotted against the absolute value of the latitude (B) of the pixels. All the synodic angular velocities have been converted into sidereal angular velocities. On the background, the grey level corresponds to the density of pixels, that is number of pixels in bins of 2 degrees in latitude by 2 degrees per day in angular velocity. The dashed line follows the maxima (per band of latitudes) of pixel density. The cloud of pixels is fitted by a function of type $f(B) = a+b*sin(B)^2+c*sin(B)^4$ (full line). For the sinusoidal polynomial fit, we found $a = 15.014 \pm 0.625, b = -3.115 \pm 2.344$, and $c = -2.866 \pm 3.906$ in degrees per day. The first value is comparable to what we know of the solar differential rotation of the bright points ($a_{bp} = 14.477 \pm 0.046$). The second coefficient is larger in magnitude than the equivalent coefficient of the bright point differential rotation ($b_{bp} = -1.84 \pm 0.41$) found by Brajša et al (2001). For the third coefficient, the error is larger than the magnitude of the coefficient: the c coefficient can not be assessed with precision. This fit of polynomial sines can also be compared with the angular speed averaged over 5-degrees bin of latitudes (Figure 3). We note a faster motion (compared to mean differential rotation) in the 15-20 deg range of latitudes, and a slower motion in the 30-35 deg range of latitudes. Latitudinal trends are qualitatively consistent with the results found by Vršnak et al (2003).

3.2. Extracting EIT Features

In order to estimate the apparent motion, we have developed a strategy of extraction of coronal regions with reliable motion. This is done by first studying the local texture of the image, within the neighborhood of each pixel. By doing so, we ensure that the intensity pattern, in terms of spatial derivatives, contains enough information so that a motion can effectively be observed and computed. In a second step, we make sure that the computed velocity is respecting our two main assumptions: brightness is constant over the neighborhood, and the velocity field is locally uniform (meaning that all the velocity vectors

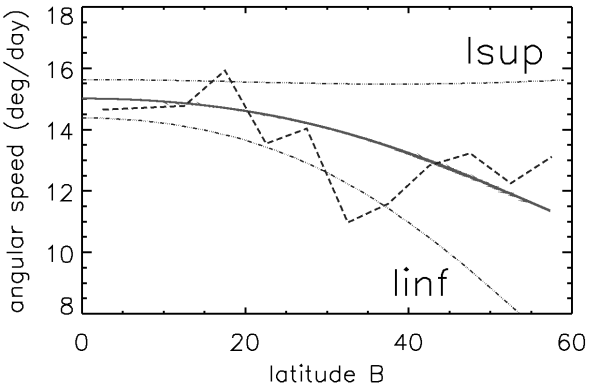

Figure 3. Full line: Fitted function of angular rotation speed. Dashed line: mean values (5-degrees bins). lsup (resp. linf): upper (resp. lower) limit of the fitted function.

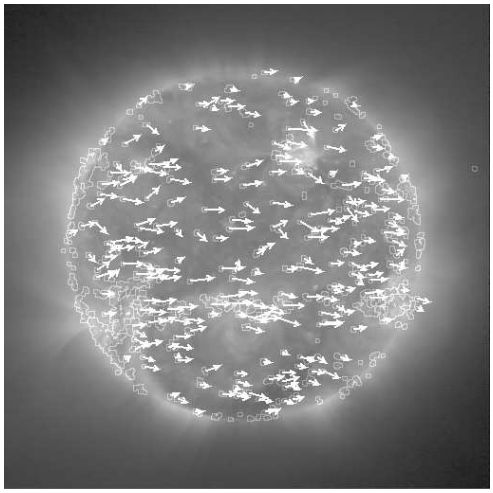

Figure 4. Extracted regions with reliable motion.

are similar in the neighborhood of the pixel). This last condition imposes the estimated velocity vector to be consistent with the temporal variation of the intensity pattern contained in the neighborhood of the pixel. We finally get a set of regions that appear to be well correlated with the small coronal objects that we would distinguish by eye (Figure 4). This is due to the selection of a sufficient spatial texture.

4. CONCLUSION

With this new method of motion analysis using optical flow technique, we derive a dense velocity field. We found that the differential rotation could be recovered on very short time scales. The velocity field of an image, estimated using only the next image in the sequence, taken 20 minutes later, exhibit on angular velocity/latitude diagrams, qualitatively and quantitatively, the differential rotation. But not all pixels are usable for a further physical interpretation. Consequently we locate the regions of the image where motion is reliably computed. For further applications, in particular the tracking of coronal objects (up to active region), we need to combine this approach with a robust but coarse motion estimation, such as spatio-temporal filtering. New aims could be considered: automated and objective analysis of the moving coronal objects, detection of transient events with outstanding motion such as coronal mass ejection (CME initiation in 19.5 nm images).

ACKNOWLEDGMENTS

The authors acknowledge the support from the Belgian government through the OSTC. SOHO is a project of international cooperation between ESA and NASA.

REFERENCES

Brajša R., Wöhl H., Vršnak B., Ruždjak V., Clette F., Hochedez J.-F., 2001, A&A 374, 309

Brajša R., Wöhl H., Vršnak B., Ruždjak V., Clette F., Hochedez J.-F., 2002, A&A 392, 329

Hochedez J.F., Jacques L., Verwichte E., Berghmans D., Wauters L., Clette, F., Cugnon P., 2001, ESA SP-477, p. 115-118

Hochedez J.-F., Jacques L., Zhukov A., Clette F., Antoine J.-P., 2002, ESA SP-508, p. 295-298

Howard R., Labonte B. J., 1980, ApJ 239, 33

Lucas B.D., Kanade T., IJCAI81, 674

November L. J., Simon G. W., 1988, ApJ 333, 427

Vršnak B., Brajša R., Wöhl H., Ruždjak V., Clette F., Hochedez J.-F., 2003, A&A 404, 1117